



## Case report

# Lymphoplasmacytic lymphoma involving the mediastinum and the lung, followed by amyloidosis: A surgically and genetically proven case

Yuichi Adachi<sup>a</sup>, Takayuki Takimoto<sup>a</sup>, Maiko Takeda<sup>b</sup>, Kinnosuke Matsumoto<sup>a</sup>, Naoko Takeuchi<sup>a</sup>, Tomoko Kagawa<sup>a</sup>, Tetsuki Sakamoto<sup>c</sup>, Takahiko Kasai<sup>b</sup>, Chikatoshi Sugimoto<sup>d</sup>, Yasushi Inoue<sup>a</sup>, Kazunobu Tachibana<sup>a,d</sup>, Toru Arai<sup>d</sup>, Yoshikazu Inoue<sup>d,\*</sup>

<sup>a</sup> Department of Internal Medicine, National Hospital Organization Kinki-Chuo Chest Medical Center, 1180 Nagasone-Cho, Kita-Ku, Sakai City, Osaka, 591-8555, Japan

<sup>b</sup> Department of Pathology, National Hospital Organization Kinki-Chuo Chest Medical Center, 1180 Nagasone-Cho, Kita-Ku, Sakai City, Osaka, 591-8555, Japan

<sup>c</sup> Department of Surgery, National Hospital Organization Kinki-Chuo Chest Medical Center, 1180 Nagasone-Cho, Kita-Ku, Sakai City, Osaka, 591-8555, Japan

<sup>d</sup> Clinical Research Center, National Hospital Organization Kinki-Chuo Chest Medical Center, 1180 Nagasone-Cho, Kita-Ku, Sakai City, Osaka, 591-8555, Japan



## ARTICLE INFO

## Keywords:

Lymphoplasmacytic lymphoma  
Amyloidosis  
MYD88 mutation  
Lymphadenopathy  
Diagnosis

## ABSTRACT

A 60-year-old man was admitted for ground glass opacity in the lower lung field and mediastinal lymphadenopathy. Blood tests revealed elevated serum IgM levels, and the urine test detected Bence-Jones protein. Surgical biopsy from the mediastinal lymph node and lung showed small lymphocytes and plasma cells between follicles, and AL kappa amyloid deposition. Genetic examination detected MYD88 L265P mutation. Our diagnosis was lymphoplasmacytic lymphoma (LPL), involving the mediastinum and the lung, followed by amyloidosis. Mutation analysis, in addition to conventional histological evaluation, was useful for a precise diagnosis.

## 1. Introduction

Lymphoplasmacytic lymphoma (LPL) is a low grade mature B cell lymphoma typically involving the bone marrow, and less commonly, the spleen and/or lymph nodes [1]. LPL accounts for about one percent of hematologic malignancies in the United States and Western Europe, and the incidence in Asia is about ten times lower [2–4]. The clinical course of LPL is indolent, and it is difficult to make a definite diagnosis because of the absence of specific morphologic, immunophenotypic, or chromosomal markers. However, recent studies have reported a diagnostic significance of MYD88 L265P mutation [5].

We herein report a patient with LPL involving the mediastinum and the lung, followed by AL type amyloidosis.

## 2. Case report

A 60-year-old man, who was treated at our hospital for chronic obstructive pulmonary disease for five years, was admitted for the

examination of ground glass opacity (GGO) in the lower lung field and mediastinal lymphadenopathy in the computed tomography (CT), which tended to be enlarged gradually. He was a former smoker (two packs a day for thirty-two years until fifty-one years of age) and had a history of surgery for inguinal hernia. He had dry cough and slight dyspnea (modified Medical Research Council [mMRC] grade I). Fine crackles were heard in the lower lung field upon chest auscultation. The superficial lymph nodes were not palpable. Laboratory data on admission are shown in Table 1.

Blood tests showed a white blood cell (WBC) count of 7400/ $\mu$ L without any significant abnormalities, hemoglobin level 14.5 g/dL, platelet count  $25 \times 10^4$ / $\mu$ L, serum total protein 6.4 g/dL, albumin 3.7 g/dL, serum creatinine 1.09 mg/dL, lactate dehydrogenase 247 IU/L, serum  $\beta$ 2-microglobulin 2.4 mg/L (reference value < 2.0 mg/L), soluble interleukin 2 receptor 469 U/mL, sialylated carbohydrate antigen Krebs von den Lungen-6 (KL-6) 805 U/mL, angiotensin-converting enzyme (ACE) level 37.4 U/L, IgM level 791 mg/dL (reference value 33–183 mg/dL), IgG level 531 mg/dL (reference value 861–1747 mg/dL), IgA level

\* Corresponding author. National Hospital Organization Kinki-Chuo Chest Medical Center, 1180 Nagasone-Cho, Kita-Ku, Sakai City, Osaka, 591-8555, Japan.

E-mail addresses: [y.adachi@imed3.med.osaka-u.ac.jp](mailto:y.adachi@imed3.med.osaka-u.ac.jp) (Y. Adachi), [takimoto.takayuki.ra@mail.hosp.go.jp](mailto:takimoto.takayuki.ra@mail.hosp.go.jp) (T. Takimoto), [takeda.maiko.jv@mail.hosp.go.jp](mailto:takeda.maiko.jv@mail.hosp.go.jp) (M. Takeda), [matsumoto.kinnosuke.hz@mail.hosp.go.jp](mailto:matsumoto.kinnosuke.hz@mail.hosp.go.jp) (K. Matsumoto), [takeuchi.naoko.hb@mail.hosp.go.jp](mailto:takeuchi.naoko.hb@mail.hosp.go.jp) (N. Takeuchi), [kagawa.tomoko.qw@mail.hosp.go.jp](mailto:kagawa.tomoko.qw@mail.hosp.go.jp) (T. Kagawa), [sakamoto.tetsuki.fs@mail.hosp.go.jp](mailto:sakamoto.tetsuki.fs@mail.hosp.go.jp) (T. Sakamoto), [kasai.takahiko.wy@mail.hosp.go.jp](mailto:kasai.takahiko.wy@mail.hosp.go.jp) (T. Kasai), [chikatoshis@gmail.com](mailto:chikatoshis@gmail.com) (C. Sugimoto), [inoue.yasushi.qn@mail.hosp.go.jp](mailto:inoue.yasushi.qn@mail.hosp.go.jp) (Y. Inoue), [tachibana.kazunobu.bk@mail.hosp.go.jp](mailto:tachibana.kazunobu.bk@mail.hosp.go.jp) (K. Tachibana), [arai.toru.cp@mail.hosp.go.jp](mailto:arai.toru.cp@mail.hosp.go.jp) (T. Arai), [giichi@me.com](mailto:giichi@me.com) (Y. Inoue).

<https://doi.org/10.1016/j.rmcr.2020.101313>

Received 29 September 2020; Received in revised form 27 November 2020; Accepted 27 November 2020

Available online 1 December 2020

2213-0071/© 2020 Published by Elsevier Ltd. This is an open access article under the CC BY-NC-ND license (<http://creativecommons.org/licenses/by-nc-nd/4.0/>).

52 mg/dL (reference value 93–393 mg/dL), and IgE level 10 IU/mL (reference value < 170 IU/mL). In the urine test, kappa type Bence-Jones proteins (BJP) were detected. Pulmonary function tests showed obstructive ventilatory impairment, forced vital capacity (FVC) 3.94 L, FVC/predicted FVC 110.4%, forced expiratory volume in 1 s (FEV<sub>1</sub>) 2.41 L, and FEV<sub>1</sub>/FVC 61.17%. Electrocardiogram and ultrasonic cardiography were normal. An enhanced chest CT revealed emphysema dominant in the upper lung field, GGO in the lower lung field, interlobular septal thickening, mediastinal lymphadenopathy, and a soft tissue shadow in the paravertebral region (Fig. 1).

A fluorodeoxyglucose (FDG)-positron emission CT examination showed FDG accumulation in ill-defined soft tissue attenuation in the mediastinum and retroperitoneum (SUV<sub>max</sub> = 2.5 and 2.4, respectively) (Fig. 2).

Bronchofiberscopy was performed. The recovery rate of bronchoalveolar lavage (BAL) from the right B<sup>5</sup> was 60.0%. A BAL fluid (BALF) evaluation showed a total cell count of 4.26 × 10<sup>5</sup>/mL and the differential WBC counts for macrophages, lymphocytes, neutrophils, and eosinophils were 95.0%, 3.8%, 0.9%, and 0.3%, respectively, showing normal proportion of the BALF. Among the T lymphocytes, the CD4/CD8 ratio was 1.8 and the proportion of CD1a was 1.3%, which was within the normal range. Bacterial, fungal, and acid-fast bacillus culture tests in BALF were negative. Transbronchial lung biopsy (TBLB) from the right S<sup>8</sup> showed the infiltration of inflammatory cells, such as lymphocytes and plasma cells, in the alveolar wall.

Due to elevated serum IgM, urinary BJP and lymphadenopathy, our differential diagnoses included LPL, mucosa associated lymphoid tissue (MALT) lymphoma with plasma cell differentiation, and multiple myeloma. Bone marrow aspiration and biopsy were performed to assess

bone marrow involvement. Normocellular marrow tissue with kappa predominant lymphocytes and plasma cells were obtained. The bone marrow smear showed 24.2% lymphocytes, 3.0% plasma cells, and some atypical cells. Flow cytometry suggested kappa-predominant B cells. These findings supported the diagnosis of LPL, but did not enable us to make a definitive diagnosis. To clarify the cause of the soft tissue shadow in the paravertebral region and GGO in the lower lung field, a surgical biopsy was performed from the right lower paratracheal lymph node and the right S<sup>8</sup> of the lung. The lymph node specimen and the surrounding connective tissue revealed small lymphocytes and plasma cells between follicles (Fig. 3A). These cells were mostly positive for CD20, CD79a, and IgM, focally positive for CD138, and negative for CD3, CD5, CD10, and CD56. A few Dutcher bodies were also observed. *In situ* hybridization (ISH) revealed immunoglobulin light-chain restriction with an elevated kappa/lambda ratio of ten (Fig. 3B and C).

DNA was extracted from paraffin-embedded tissue and a mutation analysis using an allele-specific primer-polymerase chain reaction (PCR) confirmed MYD88 L265P mutation in lymph node specimens (a substitution of leucine with proline at amino acid position 265) (Fig. 4). G-banding was not available; fluorescence *in situ* hybridization (FISH) analysis of MALT lymphoma-specific translocation was negative.

In addition, eosinophilic amorphous deposits found in the lymph nodes and stroma of the fat connective tissue stained positively by Congo red, exhibited apple green color under polarized light, and were positive for AL kappa by immunohistochemistry (Fig. 5A–D).

In the lung specimens, mild emphysema and inflammatory fibrotic changes, including fibroblastic foci, were seen in the subpleural area. Besides these changes, amyloid deposition was also confirmed in the interlobular septa, and slight plasma cell infiltration was seen around

**Table 1**  
Laboratory data on admission.

Laboratory Data								
WBC	7400	/μL	IgG	531	mg/dL	<TP-Fraction>		
Neu	68.4	%	IgA	52	mg/dL	Alb	60.2	%
Lym	21.8	%	IgM	791	mg/dL	α1	13.8	%
Mon	6.1	%	IgE	10	IU/L	α2	11.2	%
Eos	3.2	%	CEA	8.5	ng/mL	β	9.0	%
Bas	0.5	%	CYFRA	0.8	ng/mL	γ	15.8	%
RBC	471	× 10 <sup>4</sup> /μL	ProGRP	35.06	pg/mL	<Urinalysis>		
Hb	14.5	g/dL	β2-microglobulin	2.4	mg/L	Specific gravity 1.010		
Ht	42.7	%	ACE	37.4	U/L	pH	7	
Plt	25.0	× 10 <sup>4</sup> /μL	sIL-2R	469	U/mL	proteins	(-)	
TP	6.4	g/dL	KL-6	805	U/mL	occult blood	(-)	
Alb	3.7	g/dL	SP-D	101.4	ng/mL	glucose	(-)	
T-Bil	0.72	mg/dL	SP-A	49.3	ng/mL	<ABG (ambient air)>		
ALP	315	IU/L	BNP	23.5	pg/mL	pH	7.437	
AST	23	IU/L	C3	115	mg/dL	PaCO <sub>2</sub>	35.2	Torr
ALT	19	IU/L	C4	24	mg/dL	PaO <sub>2</sub>	63.9	Torr
γ-GTP	14	IU/L	<Autoimmune antibody>			HCO <sub>3</sub> <sup>-</sup>	23.3	mmol/L
LDH	247	IU/L	ANA	<40		AaDO <sub>2</sub>	46.4	Torr
CPK	152	IU/L	CCP	<0.5				
Glu	93	mg/dL	Jo-1	<0.5	U/mL			
UA	6.7	mg/dL	Scl-70	<0.6	U/mL			
BUN	10.0	mg/dL	ds-DNA	<0.7	U/mL			
Cre	1.09	mg/dL	RNP	<0.5	U/mL			
Ca	9	mg/dL	Sm	<0.5	U/mL			
CRP	0.57	mg/dL	SS-A	<0.5	IU/mL			
Na	138	mmol/L	SS-B	<0.5	IU/mL			
K	3.8	mmol/L	PR3-ANCA	<0.5	IU/mL			
Cl	107	mmol/L	MPO-ANCA	<0.5	IU/mL			

WBC, white blood cell; Neu, neutrophil; Lym, lymphocyte; Mon, monocyte; Eos, eosinophil; Bas, basophil; RBC, red blood cell; Hb, hemoglobin; Ht, hematocrit; Plt, platelet; TP, total protein; Alb, albumin; T-Bil, total bilirubin; ALP, alkaline phosphatase; AST, aspartate aminotransferase; ALT, alanine aminotransferase; γ-GTP, γ-glutamyltranspeptidase; LDH, lactate dehydrogenase; CPK, creatine phosphokinase; Glu, glucose; UA, uric acid; BUN, blood urea nitrogen; Cre, creatinine; Ca, calcium; CRP, C-reactive protein; Na, natrium (sodium); K, kalium (potassium); Cl, chlorine; CEA, carcinoembryonic antigen; CYFRA, cytokeratin 19 fragment; ProGRP, pro-gastrin releasing peptide; ACE, angiotensin converting enzyme; sIL-2R, soluble interleukin-2 receptor; KL-6, sialylated carbohydrate antigen Krebs von den Lungen-6; SP-D, surfactant protein-D; SP-A, surfactant protein-A; BNP, brain natriuretic peptide; ANA, anti-nuclear antibody; CCP, cyclic citrullinated peptide; ds-DNA, double stranded-DNA; RNP, ribonucleoprotein; Sm, smith; PR3-ANCA, serine proteinase3-anti-neutrophil cytoplasmic antibody; MPO-ANCA, myeloperoxidase-anti-neutrophil cytoplasmic antibody; ABG, arterial blood gas; PaCO<sub>2</sub>, partial pressure of arterial carbon dioxide; PaO<sub>2</sub>, partial pressure of arterial oxygen; HCO<sub>3</sub><sup>-</sup>, bicarbonate ion; AaDO<sub>2</sub>, alveolar-arterial oxygen difference.

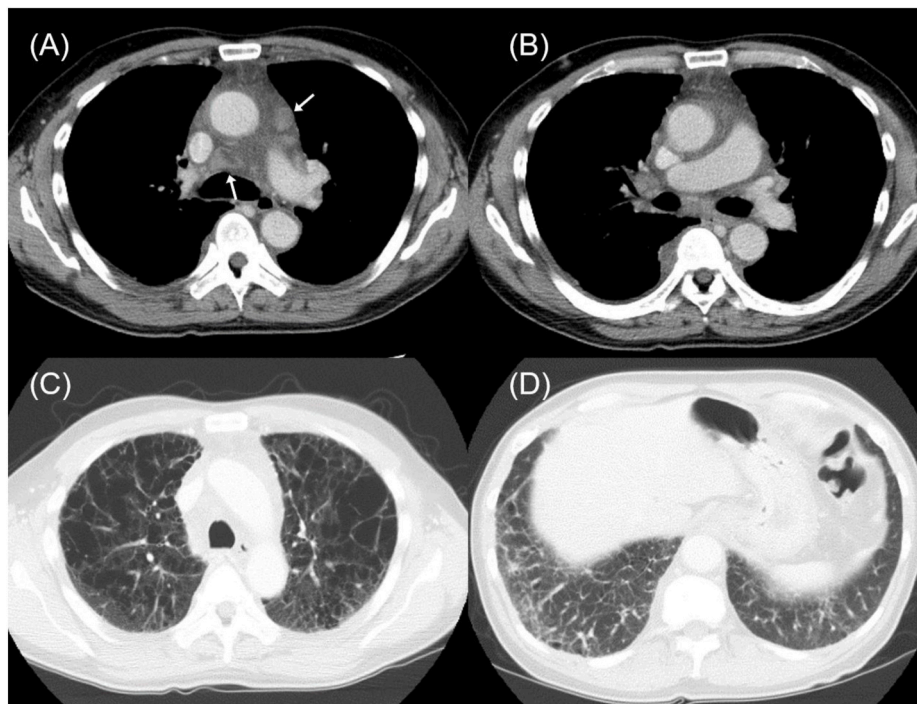


**Fig. 1.** Representative computed tomography images. Swollen lymph nodes in the mediastinum (arrows) (A), soft tissue shadow in the paravertebral region (B), centrilobular and paraseptal emphysema in the upper lobes (C), and ground glass opacities and mild reticulation (D).

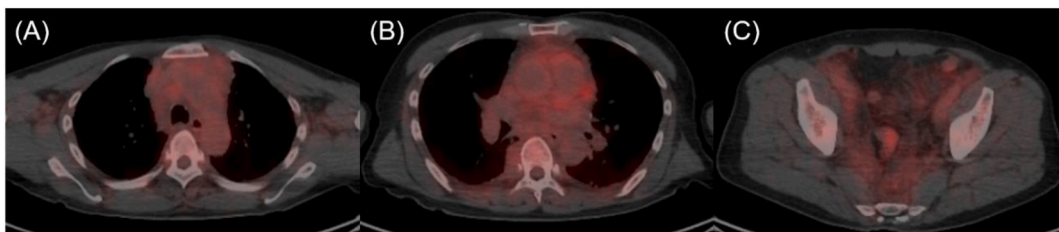


**Fig. 2.** Ill-defined soft tissue attenuation and FDG accumulation were observed in the mediastinum ( $SUV_{max} = 2.5$ ) (A), pleura (B), and retroperitoneum ( $SUV_{max} = 2.4$ ) (C).

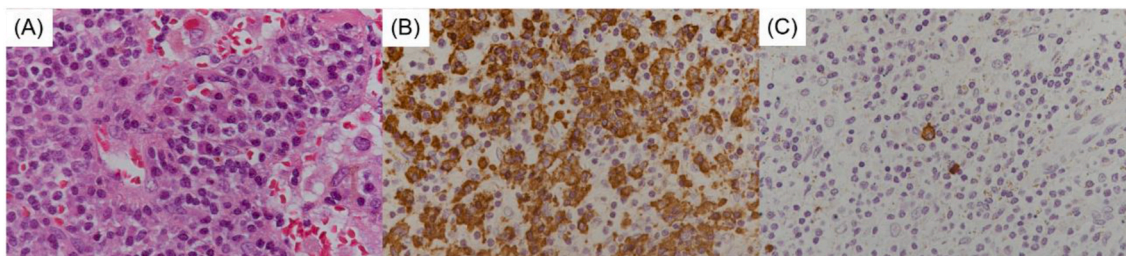


**Fig. 3.** The histology of the lymph node biopsy specimens. Infiltration of small lymphocytes and plasma cells (Hematoxylin-Eosin Staining) (A, 200 × magnification). *In situ* hybridization for immunoglobulin light chains (B, kappa; C, lambda, 200 × magnification). Most of the plasma cells were positive for immunoglobulin light chain kappa.

amyloids. Thus, LPL with AL kappa amyloidosis was diagnosed, coexisting with interstitial pneumonia with usual interstitial pneumonia (UIP) like features.

During surgical biopsy, the lung tissue and fat connective tissue were fragile and bled easily. Due to massive bleeding, the operation was changed from video assisted thoracic surgery to thoracotomy. After surgery, the patient was moved to the respiratory care unit (RCU) with intubation for 16 days because of bleeding from the airways. After his condition improved, he was referred to another hospital.

### 3. Discussion

This is a case of LPL involving the mediastinum and the lung, followed by AL type amyloidosis. The definitive diagnosis was established by pathological analysis and the detection of *MYD88* L265P mutation using surgical specimens.

The differential diagnoses included LPL, MALT lymphoma with plasma cell differentiation, plasmacytoma, and IgM monoclonal gammopathy of undetermined significance (MGUS), due to small B cell

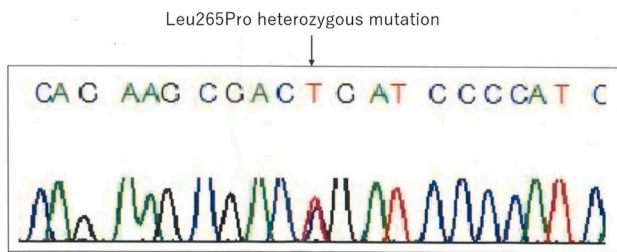


Fig. 4. MYD88 L265P mutation was detected by polymerase chain reaction with paraffin embedded tissue. Leucine (CTC) was converted to proline (CCC).

lymphoid with plasmacytic differentiation and the expression of cell surface antigens. The characteristics of these diseases are shown in Table 2 [1,6–10].

Although LPL has been recognized as a clinical entity, diagnostic criteria for lymphoplasmacytic lymphoma have always been controversial [11]. The current WHO classification defines LPL as a B-cell lymphoid neoplasm composed of small B lymphocytes, plasmacytoid

lymphocytes, and plasma cells, which does not fulfill the criteria for any of the other small B-cell lymphoid neoplasms. The diagnosis of LPL is, therefore, largely, a diagnosis of exclusion. In this case, we also detected MYD88 L265P mutation in the lymph node specimen. Previous studies have reported that this mutation can be helpful in the precise diagnosis of LPL [12–14]. MYD88 is an adaptor protein of the Toll-like receptor (TLR) pathway and MYD88 L265P mutation triggers NF-κB signaling and rapid cell proliferation [15,16]. MYD88 L265P mutation is constitutively active in lymphoma cells and that it heightens cellular proliferation and the secretion of cytokines, thereby contributing to disease progression [17]. Previous studies from multiple institutions have confirmed MYD88 L265P to be present in the majority of LPL/Waldenström Macroglobulinemia (WM), with reported incidence from 67 to 93% [5,13,18]. The mutation has also been found in 44–87% of IgM MGUS [13,18–20]. On the other hand, this abnormality has been found much less frequently in other small B-cell neoplasms, including 4–21% of cases diagnosed as MALT lymphoma, and 1–10% of chronic lymphocytic leukemia [13,18,21–23]. No MYD88 mutation was reported in plasmacytomas. In this case, we successfully diagnosed the patient as having LPL and excluded other differential diagnosis based on

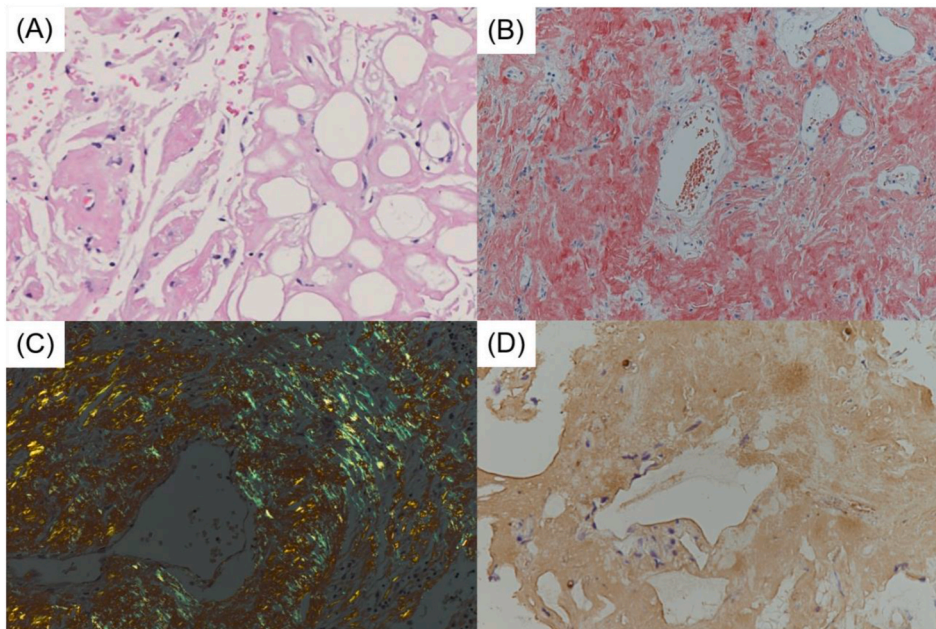


Fig. 5. The histology of the lymph node biopsy specimens. The deposition of acidophilic amorphous deposits was found in the lymph nodes (Hematoxylin-Eosin Staining) (A, 40 × magnification). Extracellular amorphous and eosinophilic deposits stained positively by Congo red (B, 40 × magnification) and exhibited apple green color under polarized light (C, 40 × magnification) and were positive for AL kappa by immunohistochemistry (D, 40 × magnification). (For interpretation of the references to color in this figure legend, the reader is referred to the Web version of this article.)

Table 2  
Characteristics of differential diagnosis.

	LPL	IgM-MGUS	MALT lymphoma	Plasmacytoma	This case
Definition	No specific cut off level of IgM Bone marrow > lymph node, spleen Usually IgM, rarely IgG or IgA	Serum IgM <30 g/L Bone marrow lymphoplasma cell <10%	Marginal zone (centrocyte-like) cells. Monocytoid B cells Bone marrow involvement (2–20%)	Monoclonal plasma cells Bone marrow clonal plasma cells ≥ 10%	Serum IgM elevated Bone marrow; lymphoplasma cells 27%
Clinical features	Symptom (+) Weakness(+) Fatigue(+) Lymphadenopathy(+)	Symptom (–) Anemia (–) Lymphadenopathy(–)	Associated with chronic immune reactions driven by bacterial, viral, or autoimmune stimuli	Symptom (+) Hypercalcemia Anemia	Lymphadenopathy (+) Anemia (–)
Histology	Monotonous small lymphocytes, plasma cells, and plasmacytoid lymphocytes CD20 (+), CD79a (+)	Bone marrow: clonal lymphoplasmacytic cells CD20 (+), CD79a (+)	Small to medium-sized B cells Plasmacytic differentiation is often present CD20(+), CD79a(+)	Monoclonal plasma cells Types of immunoglobulin; IgG > IgA > B1P CD20 (–), CD79a(+)	Small lymphocytes, plasma cells, and plasmacytoid lymphocytes IgM (+) CD20 (+), CD79a (+)
Genetic profiles	MYD88 L265P (>90%) CXCR4 (30%)	MYD88 L265P (50%) CXCR4 (20%)	API2-MALT1 (30–50%) MYD88 L265P (4–21%)	MYD88 L265P (–)	MYD88 L265P (+) MALT1 rearrangement (–)

LPL, lymphoplasmacytic lymphoma; MGUS, monoclonal gammopathy of undetermined significance; MALT, mucosa associated lymphoid tissue.

of the clinicopathological findings and *MYD88* L265P mutation.

In the current case, AL amyloidosis was also diagnosed. LPL/WM often causes secondary amyloidosis [24]. LPL/WM is associated with serum monoclonal paraprotein, usually IgM [6,25]. IgM paraprotein is implicated in 5–7% of patients with LPL [26–28]. However, the precise incidence of LPL/WM accompanied by amyloidosis is not clear. A previous study reported that 7.5% of WM patients had coexisting amyloidosis [29]. Another study reported six patients with amyloidosis associated with non-Hodgkin's lymphoma [30]. Of those six, five were LPL and the other was a small lymphocytic lymphoma with plasmacytoid features. Except for these studies, there have been no reports of the incidence of LPL/WM with amyloidosis. Therefore, we further investigated the incidence of non-Hodgkin lymphoma and amyloidosis in the lung among the cases diagnosed at our hospital. We retrospectively collected the medical records from 1993 to 2019 from the pathology department. There were twenty four cases with lymphoproliferative lung disease. Twenty-three cases were MALT lymphoma, four of which (17%) were accompanied by amyloidosis (unpublished data). The case presented here is the only one with LPL and amyloidosis. On the other hand, there were eighteen cases with amyloidosis in the lung. Among them, four cases (22%) were diagnosed as MALT lymphoma and one was LPL (5%).

#### 4. Conclusion

We encountered a case of LPL followed by amyloidosis that was definitively diagnosed by pathological analysis and the detection of *MYD88* L265P mutation using surgical specimens. Mutation analysis, in addition to conventional histological evaluation, is useful for establishing a precise diagnosis.

#### Declaration of competing interest

None.

#### Acknowledgements

The authors would like to thank Prof. K Ohashi (Yokohama City University) for the analysis of amyloid types, and Dr. T Eguchi (Osaka Minami Medical Center) and Dr. J Fujita (Osaka University Hospital) for their advice on diagnosis.

This research did not receive any specific grant from funding agencies in the public, commercial, or not-for-profit sectors.

#### References

- [1] S.H. Swerdlow, E. Campo, S.A. Pileri, et al., The 2016 revision of the World Health Organization classification of lymphoid neoplasms, *Blood* 127 (2016) 2375–2390.
- [2] L.M. Morton, S.S. Wang, S.S. Devesa, P. Hartge, D.D. Weisenburger, M.S. Linet, Lymphoma incidence patterns by WHO subtype in the United States, 1992–2001, *Blood* 107 (2006) 265–276.
- [3] M. Sant, C. Allemani, C. Tereanu, et al., Incidence of hematologic malignancies in Europe by morphologic subtype: results of the HAEMACARE project, *Blood* 116 (2010) 3724–3734.
- [4] M. Iwanaga, C.J. Chiang, M. Soda, et al., Incidence of lymphoplasmacytic lymphoma/Waldenstrom's macroglobulinaemia in Japan and Taiwan population-based cancer registries, 1996–2003, *Int. J. Canc.* 134 (2014) 174–180.
- [5] M. Varettoni, L. Arcaini, S. Zibellini, et al., Prevalence and clinical significance of the *MYD88* (L265P) somatic mutation in Waldenstrom's macroglobulinemia and related lymphoid neoplasms, *Blood* 121 (2013) 2522–2528.
- [6] N. Naderi, D.T. Yang, Lymphoplasmacytic lymphoma and Waldenstrom macroglobulinemia, *Arch. Pathol. Lab Med.* 137 (2013) 580–585.
- [7] A. Grunenberg, C. Buske, Monoclonal IgM gammopathy and waldenstrom's macroglobulinemia, *Dtsch Arztebl Int* 114 (2017) 745–751.
- [8] R.A. Kyle, D.R. Larson, T.M. Therneau, et al., Long-term follow-up of monoclonal gammopathy of undetermined significance, *N. Engl. J. Med.* 378 (2018) 241–249.
- [9] A. Ambrosetti, R. Zanotti, C. Pattaro, et al., Most cases of primary salivary mucosa-associated lymphoid tissue lymphoma are associated either with Sjogren syndrome or hepatitis C virus infection, *Br. J. Haematol.* 126 (2004) 43–49.
- [10] R. Soutar, H. Lucraft, G. Jackson, et al., Guidelines on the diagnosis and management of solitary plasmacytoma of bone and solitary extramedullary plasmacytoma, *Br. J. Haematol.* 124 (2004) 717–726.
- [11] P. Lin, L.J. Medeiros, Lymphoplasmacytic lymphoma/waldenstrom macroglobulinemia: an evolving concept, *Adv. Anat. Pathol.* 12 (2005) 246–255.
- [12] S.P. Treon, L. Xu, G. Yang, et al., *MYD88* L265P somatic mutation in Waldenstrom's macroglobulinemia, *N. Engl. J. Med.* 367 (2012) 826–833.
- [13] C. Jimenez, E. Sebastian, M.C. Chillón, et al., *MYD88* L265P is a marker highly characteristic of, but not restricted to, Waldenstrom's macroglobulinemia, *Leukemia* 27 (2013) 1722–1728.
- [14] F. Hamadeh, S.P. MacNamara, N.S. Aguilera, S.H. Swerdlow, J.R. Cook, *MYD88* L265P mutation analysis helps define nodal lymphoplasmacytic lymphoma, *Mod. Pathol.* 28 (2015) 564–574.
- [15] N. Warner, G. Nunez, *MyD88*: a critical adaptor protein in innate immunity signal transduction, *J. Immunol.* 190 (2013) 3–4.
- [16] G. Yang, Y. Zhou, X. Liu, et al., A mutation in *MYD88* (L265P) supports the survival of lymphoplasmacytic cells by activation of Bruton tyrosine kinase in Waldenstrom macroglobulinemia, *Blood* 122 (2013) 1222–1232.
- [17] S.M. Ansell, L.S. Hodge, F.J. Secreto, et al., Activation of *TAK1* by *MYD88* L265P drives malignant B-cell Growth in non-Hodgkin lymphoma, *Blood Canc. J.* 4 (2014) e183.
- [18] L. Xu, Z.R. Hunter, G. Yang, et al., *MYD88* L265P in Waldenstrom macroglobulinemia, immunoglobulin M monoclonal gammopathy, and other B-cell lymphoproliferative disorders using conventional and quantitative allele-specific polymerase chain reaction, *Blood* 121 (2013) 2051–2058.
- [19] N. Gachard, M. Parrens, I. Soubeyran, et al., IGHV gene features and *MYD88* L265P mutation separate the three marginal zone lymphoma entities and Waldenstrom macroglobulinemia/lymphoplasmacytic lymphomas, *Leukemia* 27 (2013) 183–189.
- [20] O. Landgren, L. Staudt, *MYD88* L265P somatic mutation in IgM MGUS, *N. Engl. J. Med.* 367 (2012) 2255–2256.
- [21] L. Wang, M.S. Lawrence, Y. Wan, et al., *SF3B1* and other novel cancer genes in chronic lymphocytic leukemia, *N. Engl. J. Med.* 365 (2011) 2497–2506.
- [22] A. Martinez-Trillos, M. Pinyol, A. Navarro, et al., Mutations in *TLR/MyD88* pathway identify a subset of young chronic lymphocytic leukemia patients with favorable outcome, *Blood* 123 (2014) 3790–3796.
- [23] X.S. Puente, M. Pinyol, V. Quesada, et al., Whole-genome sequencing identifies recurrent mutations in chronic lymphocytic leukaemia, *Nature* 475 (2011) 101–105.
- [24] M.A. Gertz, R.A. Kyle, P. Noel, Primary systemic amyloidosis: a rare complication of immunoglobulin M monoclonal gammopathies and Waldenstrom's macroglobulinemia, *J. Clin. Oncol.* 11 (1993) 914–920.
- [25] M.A. Gertz, Waldenstrom macroglobulinemia: 2019 update on diagnosis, risk stratification, and management, *Am. J. Hematol.* 94 (2019) 266–276.
- [26] M.A. Gertz, F.K. Buadi, S.R. Hayman, IgM amyloidosis: clinical features in therapeutic outcomes, *Clin. Lymphoma, Myeloma & Leukemia* 11 (2011) 146–148.
- [27] A.D. Wechalekar, H.J. Lachmann, H.J. Goodman, A. Bradwell, P.N. Hawkins, J. D. Gillmore, AL amyloidosis associated with IgM paraproteinemia: clinical profile and treatment outcome, *Blood* 112 (2008) 4009–4016.
- [28] G. Palladini, P. Russo, T. Bosoni, et al., AL amyloidosis associated with IgM monoclonal protein: a distinct clinical entity, *Clin Lymphoma Myeloma* 9 (2009) 80–83.
- [29] S. Zanwar, J.P. Abeykoon, S.M. Ansell, et al., Primary systemic amyloidosis in patients with Waldenstrom macroglobulinemia, *Leukemia* 33 (2019) 790–794.
- [30] Cohen AD, Zhou P, Xiao Q et al. Systemic AL amyloidosis due to non-Hodgkin's lymphoma: an unusual clinicopathologic association. *Br. J. Haematol.* 124:309–314, 200.